

## Fabrication of Alginate-Based Electrospun Nanofibers for Carbon Dioxide Removal

Adhitasari Suratman<sup>1\*</sup>, Desi Nur Astuti<sup>1</sup>, Ryan Jonathan<sup>1</sup>, Agus Kuncaka<sup>1</sup>, and Yusril Yusuf<sup>2</sup>

<sup>1</sup>Department of Chemistry, Faculty of Mathematics and Natural Sciences, Universitas Gadjah Mada, Sekip Utara, Yogyakarta 55281, Indonesia

<sup>2</sup>Department of Physics, Faculty of Mathematics and Natural Sciences, Universitas Gadjah Mada, Sekip Utara, Yogyakarta 55281, Indonesia

\* **Corresponding author:**

email: adhitasari@ugm.ac.id

Received: July 6, 2021

Accepted: January 26, 2022

DOI: 10.22146/ijc.67349

**Abstract:** A fabrication of eco-friendly and low-cost adsorbent materials is reported for CO<sub>2</sub> removal. Alginate nanofibers (NFs) adsorbents were prepared by incorporating poly(vinyl alcohol) (PVA) into alginate solutions via electrospinning technique from alginate biopolymers. Smooth-surfaced Alg/PVA NFs were obtained with a specific surface area of 9.197 m<sup>2</sup> g<sup>-1</sup>. Zeolite (Z) was impregnated into polymer solutions to enhance the properties and performances of alginate nanofibers. Alg/PVA/Z NFs appeared to be rougher with a specific surface area of 25.998 m<sup>2</sup> g<sup>-1</sup>. Both adsorbents offered great potential for CO<sub>2</sub> adsorbent in the future. The adsorption isotherms of Alg/PVA NFs followed the Langmuir model with optimum CO<sub>2</sub> adsorption capacity of 3.286 mmol g<sup>-1</sup> and Alg/PVA/Z NFs followed Dubinin-Radushkevich model with optimum CO<sub>2</sub> adsorption capacity of 10.710 mmol g<sup>-1</sup>.

**Keywords:** electrospinning; nanofibers; alginate; poly(vinyl alcohol) (PVA); zeolites; carbon dioxide

### ■ INTRODUCTION

Over the past decades, fossil fuel combustion has elevated the atmospheric CO<sub>2</sub> concentration up to 416.87 ppm as of December 2021 [1]. Excessive release of carbon dioxide leads to global warming, which causes a threat to the environment and public health. Hence, it is essential to reduce carbon emissions. Carbon Capture and Separation (CCS) is a main technology for managing and mitigating CO<sub>2</sub> emissions. There are several pathways for CCS, such as pre-combustion, post-combustion, and oxy-fuel combustion [2]. Post-combustion is currently the most favored approach for capturing CO<sub>2</sub>. Several post-combustion methods are available, including adsorption, absorption, membrane, and cryogenic. Among various methods, adsorption is preferable due to its cost-effective process, high CO<sub>2</sub> adsorption capacity, and low-energy requirement. Many studies have been conducted to develop adsorbent materials for carbon capture, such as carbonaceous materials (activated carbons, carbon nanotubes, graphene), biochar, zeolites, Metal-Organic

Frameworks (MOFs), Zeolitic Imidazolate Frameworks (ZIFs), and nanomaterials [2].

Nanomaterials, such as nanofibers offer higher specific surface area, which have a high potential for carbon dioxide removal. There are various fabrication methods to produce nanofibers, however, electrospinning is currently the most versatile technique for manufacturing nanofibers on an industrial scale. Electrospinning involves the electrohydrodynamic principle, in which a droplet of liquid is electrified to form a jet, followed by stretching and elongation to form nanofibers [3].

Electrospun nanofibers have exhibited prospective properties as adsorbent materials for carbon capture owing to their high porosity, high specific surface area, unique structure, good interconnectivity, tunable pore size, good mechanical properties, low gas resistance, and rapid kinetics reaction [3]. Various electrospun nanofibers adsorbent have been developed for CO<sub>2</sub> adsorption from diverse materials such as biopolymers [4-5], synthetic polymers [6-9], carbons [10-14], MOFs

[15-16], amine sorbents [17-18], metals oxides and ceramics [19-20].

In the past years, biopolymers-based adsorbents such as alginate have gained immense interest due to increased ecological and environmental concerns. Alginate consists of linear unbranched anionic polysaccharides of (1-4)-linked  $\beta$ -D-mannuronic acid (M) and  $\alpha$ -L-guluronic acid (G) monomers which can be extracted from seaweed, specifically alginophyte seaweed species [21]. Seaweed cultivations are dominated by Asian countries, in which Indonesia is the major producers alongside China, Japan, Korea, and the Philippines. In 2016, Indonesia was listed as the second-largest seaweed producers with 38.7% of the global production, only topped up by China with 47.9% [22]. According to Presidential Regulation No. 33/2019, Indonesia has the potential to cultivate seaweed on 1.5 million hectares, in which estimation of alginophyte seaweed production can reach more than 240 thousand tons per year. Taking advantage of the abundant seaweed resources, the alginate can be one alternative of biodegradable biopolymers, low-cost sources, and generally non-toxic to the environment [23].

Alginate has been investigated for various applications, including CO<sub>2</sub> adsorption, because of its high hydrophilicity resulting from its hydroxyl and carboxyl groups [24]. Since alginate is polyelectrolyte, it is quite challenging to produce electrospun nanofibers from pure alginate solutions. However, these restrictions and processing limitations can be improved by introducing carrier copolymers into the alginate solution. One of the most commonly used copolymers is poly(vinyl alcohol) (PVA). PVA is a semi-crystalline hydrophilic polymers that is biocompatible with alginate, non-toxic, biodegradable, with thermal stability, and many carbonyl groups that can bind carbon dioxide molecules [21,25-26].

Another adsorbent that also has been broadly studied for CO<sub>2</sub> removal is zeolites. Zeolites are microporous crystalline aluminosilicate minerals that consist of silicate [SiO<sub>4</sub>]<sup>4-</sup> and aluminate [AlO<sub>4</sub>]<sup>5-</sup> tetrahedrons connected by oxygen atoms, forming a box-like structure with a molecular size of 0.5–1.2 nm. Zeolite exhibits excellent carbon capture performance as it has

high CO<sub>2</sub> adsorption capacity and selectivity at low pressure. Nevertheless, zeolite is very sensitive in the presence of water or moisture that causes greatly downgrade for CO<sub>2</sub> adsorption [27].

For long periods of time, zeolites have been exploited for environmental remediation with remarkable adsorption capacity, and yet, the materials classified as non-renewable resources that could generate secondary pollutant. On the other hands, alginate has been under spotlighted for carbon dioxide discharge since it is contained abundant hydroxyl and carboxyl groups also naturally biodegradable. Nonetheless, alginate performance still needed some improvement. Zeolites and alginate have been separately applied as CO<sub>2</sub> adsorbents, therefore, this study focused on combining extensive resources of alginate in Indonesia with natural zeolites obtained from local mining to synthesize eco-friendly carbon dioxide adsorbents. Afterward, an electrospinning technique was performed to fabricate alginate-zeolite nanofibers. Recently, utilizing nano-size zeolites have been reported. Many researchers have successfully fabricated zeolites nanofibers using the electrospinning technique [28-36]. Zeolites nanofibers have exhibited several advantages such as better performance and lifetime, improved mass transfer, higher selectivity, and minimized recovery and agglomeration issues [32].

## ■ EXPERIMENTAL SECTION

### Materials

Na-Alginate (medium viscosity, vis.  $\geq$  2000 cps), poly(vinyl alcohol) (PVA) (ave. Mw 70000–100000, fully hydrolyzed, vis. 11–14 cps), natural zeolite from Klaten (Central Java, Indonesia), HNO<sub>3</sub> 70%, Na<sub>2</sub>EDTA 1 M, NaOH, HCl 37%, Sodium tetraborate (Na<sub>2</sub>B<sub>4</sub>O<sub>7</sub>·10H<sub>2</sub>O), CO<sub>2</sub> gas, phenolphthalein and methyl orange indicators. All chemicals and solvents were procured from Merck and Sigma Aldrich in pro-analytical grade and used as received without further purification.

### Instrumentation

The electrospinning technique is set at 15 kV with a tip-to-collector distance of 15 cm at room temperature.

Conductivity-meter used is from ST10C-B (Ohaus). The Fourier transform infrared (FT-IR) used is from Shimadzu-Prestige 21 using the KBr pellet technique. Scanning Electron Microscopy-Energy Dispersive Spectroscopy (SEM-EDS) is from JEOL JSM-6510LA. Surface Area & Pore Size Analyzer is from Quantachrome Nova 1200e. CO<sub>2</sub> adsorption was investigated using a gas trapping system (Fig. 1).

## Procedure

### Synthesis Alg/PVA NFs

Alg/PVA NFs were synthesized following the procedure described by Islam and Karim (2010) [37]. Alg/PVA solutions were prepared by stirring alginate solution (2% w/w in double distilled water/DDW) and PVA solution (10% w/w in DDW) in various volume ratios (0:10, 1:9, 2:8, 3:7, and 4:6 v/v) for 2 h at room temperature. Alg/PVA solutions were electrospun for 2 h and collected on a grounded collector. As-spun Alg/PVA NFs were dried at room temperature and characterized using FTIR, SEM, and Surface Area & Pore Size Analyzer.

### Synthesis zeolites modified Alg/PVA nanofibers (Alg/PVA/Z NFs)

Natural zeolite sieved 170 was demineralized by Na<sub>2</sub>EDTA for 24 h and dealuminated using 8 M HNO<sub>3</sub> in water for 24 h. The pretreated zeolite was activated by calcination at 500 °C at a rate of 10 °C/min for 3 h in the air. Alg/PVA/Z NFs were fabricated by impregnating activated zeolites to the Alg/PVA solutions (2:8 v/v) with a various mass of zeolites 0.5–3.0% (w/w). The mixtures were electrospun for 2 h and collected on a grounded collector. As-spun Alg/PVA/Z NFs were dried at room temperature and characterized using FTIR, SEM, and Surface Area & Pore Size Analyzer.

### Carbon dioxide capture

The capturing CO<sub>2</sub> gas was carried out using a gas trapping system at ambient temperature and pressure 1 atm (see Fig 1). The adsorption capacity of Alg/PVA NFs and Alg/PVA/Z NFs were analyzed by titrimetric method, in which carbon dioxide gas was trapped with NaOH solution. Initially, CO<sub>2</sub> gas was passed through the gas trapping system at a specific flow rate (10–50 mL min<sup>-1</sup>) for a period of time (10–30 min) without the adsorbent

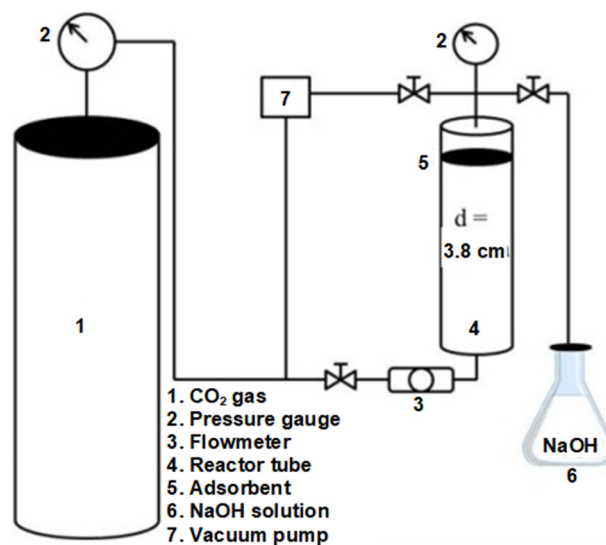


Fig 1. CO<sub>2</sub> adsorption process using gas trapping system

material. Afterward, Alg/PVA NFs and Alg/PVA/Z NFs adsorbent were placed in the reactor tube. Carbon dioxide then flowed into the reactor chamber at the same condition. The uncaptured CO<sub>2</sub> was trapped in NaOH 0.1 M and formed as Na<sub>2</sub>CO<sub>3</sub>. NaOH was titrated with HCl 0.1 M, and the concentration of uncaptured CO<sub>2</sub> was analyzed using back titration (Warder's method). Adsorption capacity of As-spun Alg/PVA NFs and Alg/PVA/Z NFs were conducted with various flowrates (10, 20, 30, 40, and 50 mL min<sup>-1</sup>), contact time (10, 15, 20, 25, and 30 min), basis weight (i.e. electrospun time 1, 2, 3, 4, and 5 h), and mass of zeolites (0.5, 1.0, 1.5, 2.0, 2.5, and 3.0% (w/w)). The adsorption behaviors were analyzed using Langmuir, Freundlich, Dubinin-Radushkevich (DR), Temkin, and Elovich isotherm models (Table S2). The adsorption isotherm was studied using collected data for gas flowrates versus adsorption capacity.

## RESULTS AND DISCUSSION

### FTIR Characterization

As shown in Fig. 2, alginate showed characteristic peaks at 1033, 1419, 1635, and 3448 cm<sup>-1</sup> corresponding to the stretching of –C–O–C, symmetric –COO–, asymmetric –COO–, and O–H, respectively. The characteristic bands of pristine PVA were observed at 848 cm<sup>-1</sup> (C–H isotactic stretching), 1095 cm<sup>-1</sup> (C–O stretching), 1342 cm<sup>-1</sup> (C–H stretching), 1442 cm<sup>-1</sup>

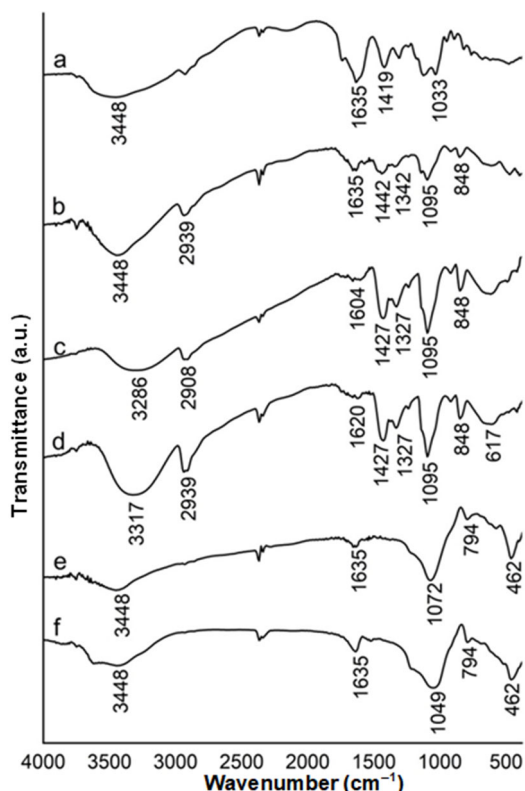


**Fig 2.** FTIR spectra of alginate (a), PVA (b), as-spun Alg/PVA NFs 2:8 (c), as-spun Alg/PVA/Z NFs 2:8:2.5 (d), activated zeolites (e), and natural zeolites (f)

(symmetric  $\text{-COO-}$  stretching),  $1635\text{ cm}^{-1}$  (C–O stretching from acetate group),  $2939\text{ cm}^{-1}$  ( $\text{CH}_2$  stretching), and  $3448\text{ cm}^{-1}$  (O–H stretching) [38]. Natural zeolites exhibited peaks at  $462\text{ cm}^{-1}$  for bending vibration of O–Si–O,  $794\text{ cm}^{-1}$  corresponds to an allotropic phase of  $\text{SiO}_2$ . The vibration of Al–O bonds were shown at  $1049\text{ cm}^{-1}$ . A band at  $1635\text{ cm}^{-1}$  was associated with the Si–O bond. Hydroxyl groups were shown at  $3448\text{ cm}^{-1}$ . After pretreatment, activated zeolites were seen with similar spectra of natural zeolites, but the Al–O vibration band shifted to  $1072\text{ cm}^{-1}$ , indicating that the dealumination was successfully performed [39-40].

All as-spun Alg/PVA NFs exhibit similar bands as alginate and PVA, however, a few changed vibrations. For instance, Alg/PVA NFs 2:8 (Fig. 2(a)), O–H and C–O carbonyl stretching vibration shifted to lower band numbers at  $3286$  and  $1604\text{ cm}^{-1}$ , respectively. These phenomena attributed to the fact that intermolecular interactions through hydrogen bonding between the

hydroxyl group of alginate and the etheric oxygen of PVA occurred (Fig. 3) [38]. The presence of zeolites in alginate-based nanofibers was represented by the bands in the range of  $400\text{--}700\text{ cm}^{-1}$  for zeolites structural unit and  $1620\text{ cm}^{-1}$  for Si–O bonds. Overall, as-spun Alg/PVA/Z NFs were also displayed to be shifted. Alg/PVA/Z NFs 2:8:2.5 showed the broadened peak of O–H stretching vibration was at lower wavenumber of  $3317\text{ cm}^{-1}$  (the detailed assignment bands summarized in Table S1). This phenomenon could indicate that zeolite was interacted with alginate-PVA by polymers intermolecular interaction. Si(Al)–O from zeolites and O–H groups of PVA as well as alginate backbone interacted *via* hydrogen bonding (Fig. 4) [28,34].

### Effect of Polymer Characteristic and Conductivity on Nanofibers Formation

There are three parameters that control the

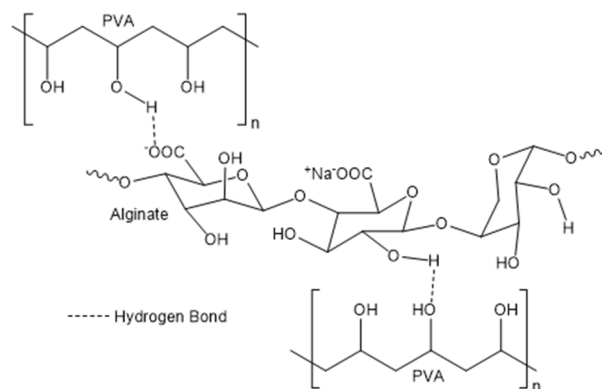


**Fig 3.** Illustrated representation of alginate-PVA intermolecular interactions

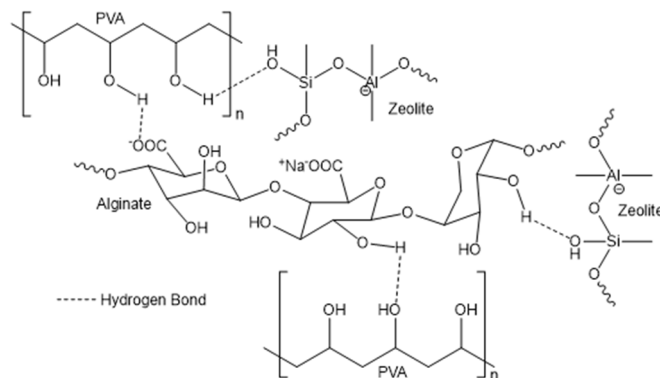


**Fig 4.** Illustrated representation of alginate-PVA-zeolites intermolecular interactions

dimension, structure, and morphology of nanofibers: solution, process, and ambient parameters. The parameters of solution were determined by polymer characteristics and solvents, such as polymer type, molecular weight, concentration, viscosity, surface tension, conductivity, and dielectric constant [41]. Natural polymers such as alginate were difficult to electrospin. The main reasons were due to polyelectrolyte character and low conductivity of pure alginate solution, as shown in Fig. 5 (volume ratio alginate to PVA of 10:0).

During the electrospinning process, polymer solution was fed into the syringe and ejected out as a spherical-shape droplet at the tip of the spinneret. A high voltage was applied to the droplet. When the electric field reached a certain threshold, the droplet was converted into a conical shape (i.e. Taylor cone). However, alginate solution could not be formed as a stable droplet. Polyelectrolyte character induced strong electrostatic repulsion that deformed the shape of the droplet and therefore inhibited the formation of Taylor cone. When the intensity of high voltage was increased, the repulsive

electrostatic forces overcame the surface tension, and the Taylor cone was then generated into a charged jet and thin fiber formed. However, polymers with low conductivity character lacked surface charge, which resulted in jet instability [3,21,41]. From the aforementioned explanations, it can be concluded that pure alginate solutions could not support electrospun and resulted in droplets form (Fig. 6(a)).

The formation of nanofibers can be improved by

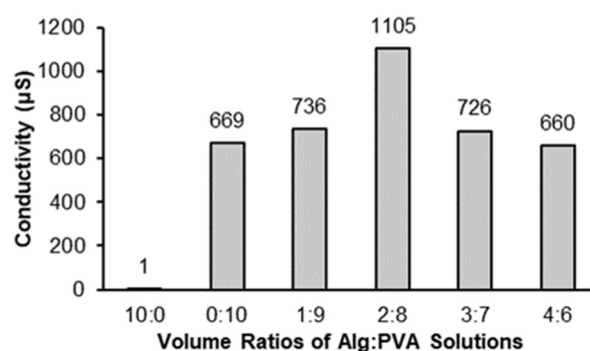


Fig 5. Conductivity values of various alginate/PVA solutions

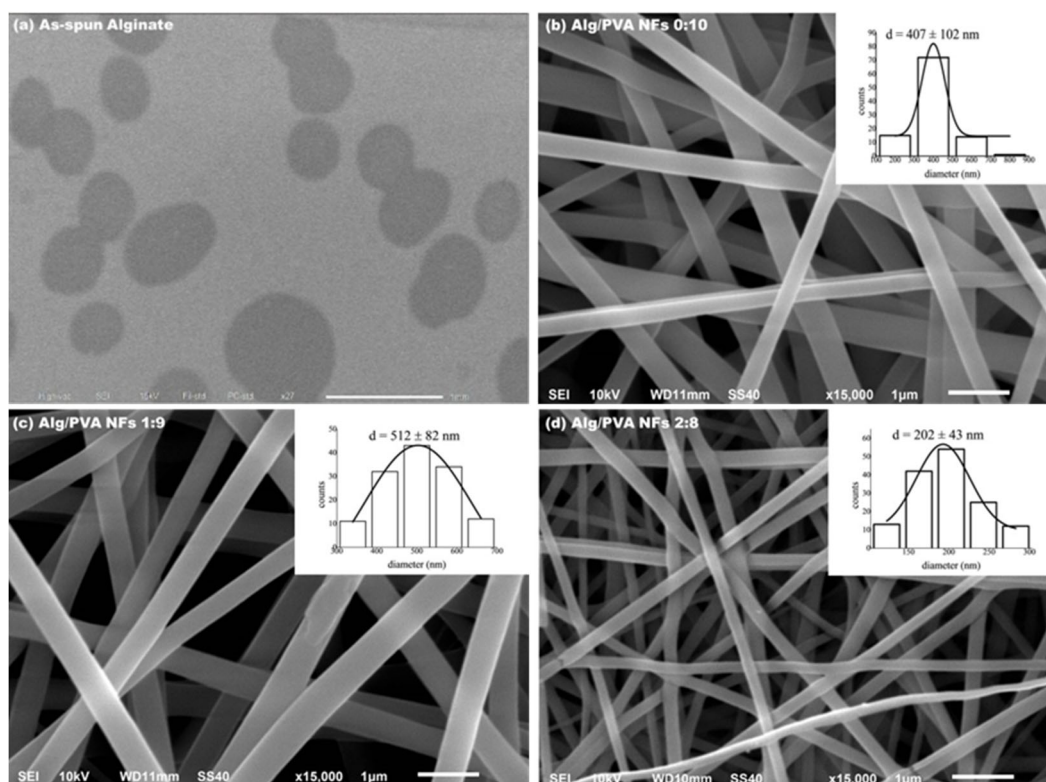
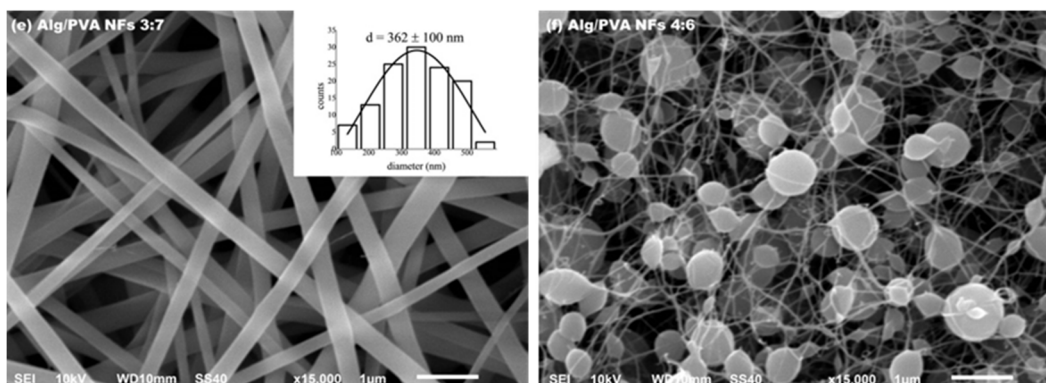


Fig 6. SEM images of as-spun alginate (a), as-spun Alg:PVA NFs volume ratios 0:10 (b), 1:9 (c), 2:8 (d), 3:7 (e), and 4:6 (f); insets show diameter of each nanofibers



**Fig 7.** SEM images of as-spun alginate (a), as-spun Alg:PVA NFs volume ratios 0:10 (b), 1:9 (c), 2:8 (d), 3:7 (e), and 4:6 (f); insets show diameter of each nanofibers (*Continued*)

introducing PVA into alginate solutions. The Addition of copolymer reduced repulsion forces among polyanionic alginate molecules by breaking hydrogen bonds within alginate chains and thus enabled the formation of alginate nanofibers. PVA incorporation also increased solution conductivity because intermolecular bonds between alginate and PVA can lessen the rigidity of three-dimension structure and enhance the mobility of alginate chains [25-26]. Incorporated PVA into alginate solution with volume ratios Alg to PVA of 0:10, 1:9, 2:8, and 3:7 formed beadless nanofibers (Fig. 6(b-e)), but further increase alginate loading beyond that (4:6) resulted in beaded nanofibers (Fig. 6(f)) due to the dominance of polyelectrolyte nature of alginate solution. The most uniform, continuous, smooth-surfaced, and thinnest Alg/PVA NFs were obtained from Alg:PVA solution volume ratio 2:8 with an average diameter of  $202 \pm 43$  nm.

### Impregnation Porous Material on Electrospun Nanofibers

Impregnation of zeolite particles into Alg/PVA solutions disrupted the dynamic interactions within alginate and PVA and changed solution characteristics. When the amount of added zeolites increased, conductivity values gradually decreased (Fig. 7). Lower conductivity reduced the ability of the solutions to carry sufficient charges for nanofibers formation, as a result Alg/PVA/Z NFs appeared to be rougher and bigger in diameter, which can be seen in SEM analysis (Fig. 8(a,c,e)). Elemental analysis of Alg/PVA/Z NFs was carried out using SEM-EDS (Fig. 8(b,c,f)), revealing that

zeolites embedded into nanofibers structure. Mass percentage of particles increased as more zeolite was added into the solution. The high content of zeolites also generated lumps alongside nanofibers because of the particles aggregation [28-29,33,36]. The highest content of zeolites with minimized agglomeration and uniform Alg/PVA/Z NFs was obtained from a solution with a zeolite mass of 2.5% (w/w) with an average diameter of  $250 \pm 60$  nm.

### CO<sub>2</sub> Adsorption of Alginate-Based Nanofibers

The performance of Alg/PVA NFs for carbon capture was evaluated by varying morphologies, gas flowrates, contact times, and basis weight of the adsorbent. There are three different structural morphologies of nanofibers, namely smooth fiber, beads-on-string, and beads, in which affected the adsorption capacity of the materials. In respect to investigating the dependence of nanofiber morphologies

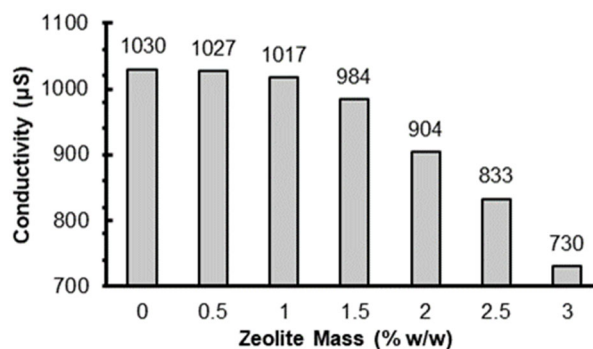


**Fig 8.** Conductivity values of alginate-PVA solution with different loading of zeolite particles

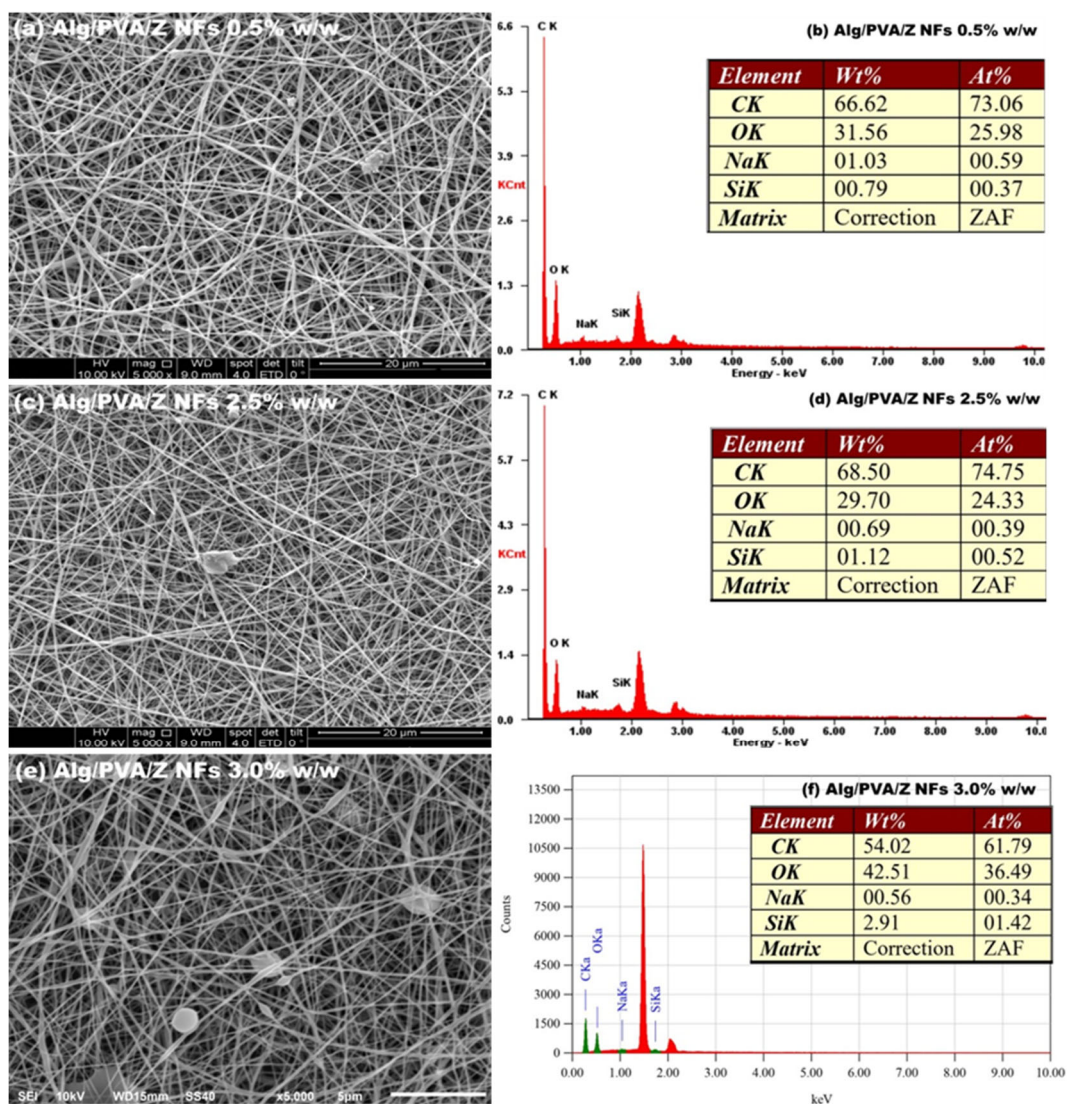


**Fig 9.** SEM images and EDX analysis of as-spun Alg/PVA/Z NFs with various zeolites mass: 0.5 (a, b), 2.5 (c, d), and 3.0 (e, f) % w/w

in CO<sub>2</sub> removal, a series of variation volume ratios alginate solution to PVA solution was conducted. As stated in the previous discussion, Alg/PVA NFs 0:10, 1:9, 2:8, and 3:7 formed beadless and smooth fiber morphology. As shown in Fig. 9(a), Alg/PVA NFs 2:8 with the finest diameter exhibited the largest adsorption capacity at 3.286 mmol g<sup>-1</sup>. Apparently, thinner nanofibers had a higher total surface area, which influenced their enhanced ability to capture submicron particles and increased the higher filtration efficiency [42].

Pressure was another aspect that needed to be taken into consideration in carbon dioxide removal, which can

be achieved by varying flowrate (Fig. 9(b)) and contact time (Fig. 9(c)). Higher flowrate and contact time led to higher gas pressure inside reactor tube which caused lower adsorption capacity. High pressure tended to increase desorption rate over adsorption rate. The best flowrate and contact time about 20 mL min<sup>-1</sup> and 20 min, respectively. Additionally, adsorbent mass also influenced the CO<sub>2</sub> uptake. Mass of the resulted nanofibers is measured by basis weight, mass per unit area of the material. Variation of electrospun time (1, 2, 3, 4, and 5 h) could alter the basis weight of Alg/PVA NFs. When the basis weight was increased until 4955 g m<sup>-2</sup> (electrospun

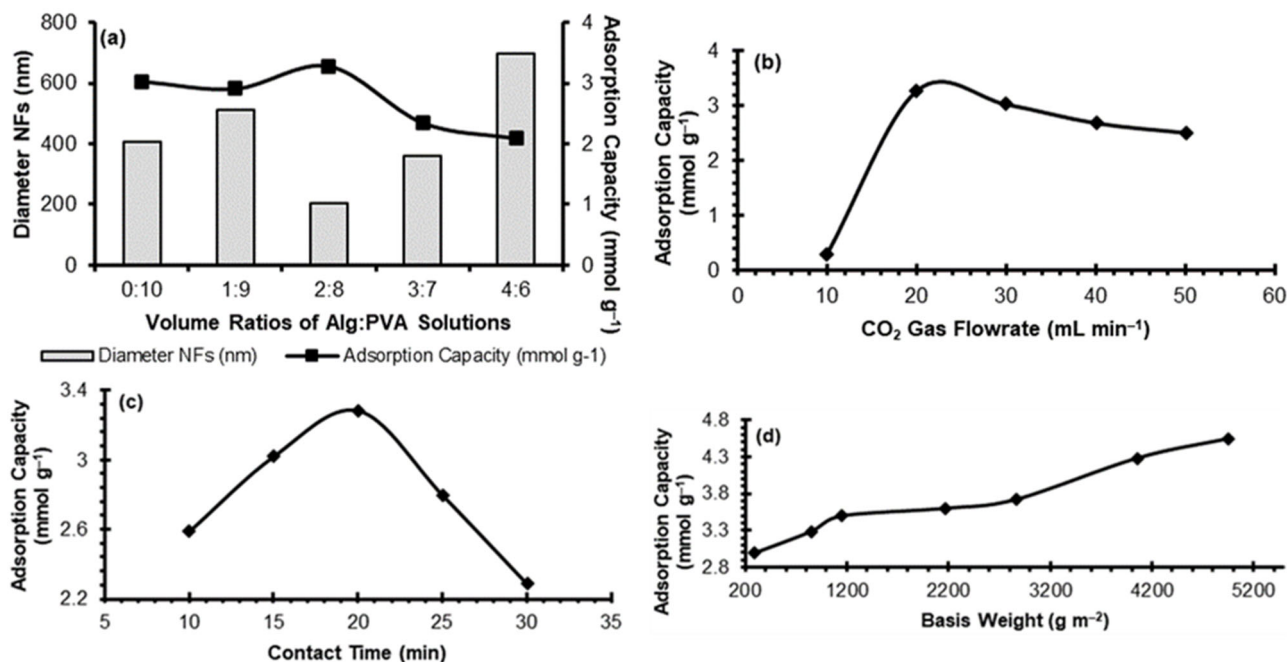


**Fig 10.** Adsorption capacity of Alg/PVA NFs 2:8 with various volume ratios of Alg/PVA solution (a), gas flowrate (b), contact time (c), and basis weight (d). All analysis carried out at ambient temperature and pressure 1 atm

time 5 h), the adsorption capacity increased up to 4.548 mmol g<sup>-1</sup> because the more enormous basis weight made the adsorbent denser and provided more active sites [43].

### Influence of Zeolites on Adsorption Capacity

The specific surface area was a critical factor in carbon capture, hence zeolites were added into Alg/PVA solutions. Zeolites are well-known adsorbents for CO<sub>2</sub> removal. Zeolites properties and performances are affected by their particle sizes. When presented in nanoscale, zeolites have higher external surface area and more accessible active sites, therefore their performances would increase [31]. The adsorption capacities of

Alg/PVA/Z NFs were gradually enhanced with increase in zeolites loading. The maximum capacity was 10.710 mmol g<sup>-1</sup> which obtained from zeolites mass 2.5% (w/w). Further increase of zeolites load led to decreased in CO<sub>2</sub> adsorption capacity (Fig. 10(a)). High contains of zeolites produced beaded nanofibers with lower specific surface area and porosity of the resulted nanofibers. Zeolites were suitable adsorbents for low to moderate pressure. Therefore, raising gas flow rates created higher pressure conditions, resulting in decreased adsorption capacity due to the weak interaction between adsorbent-adsorbate became unstable. It led to more desorption of carbon dioxide molecules (Fig. 10(b)) [40].

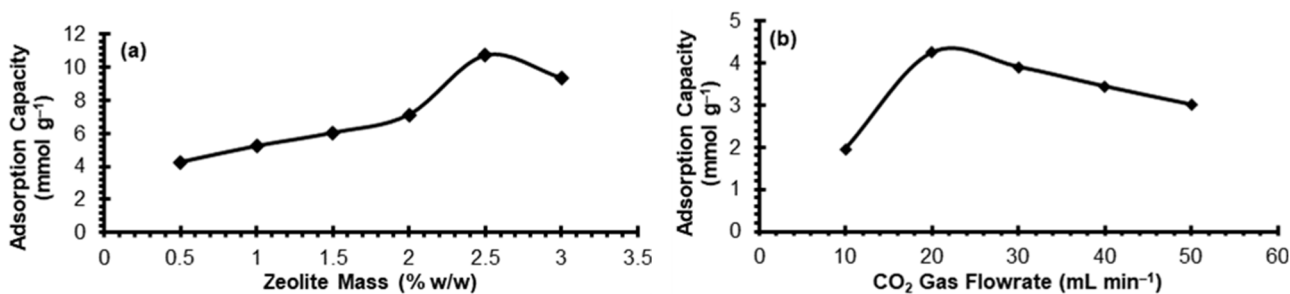


**Fig 11.** Adsorption capacity of Alg/PVA/Z NFs 2:8:2.5 with various zeolites loading (a) and gas flowrate (b). All experiments were done at ambient temperature and pressure 1 atm

In order to evaluate specific surface area of the adsorbents,  $N_2$  adsorption isotherm were carried out at 77 K. As shown in Fig. 11, alginate-based nanofiber adsorbents exhibit Type I isotherm that indicating the typical microporous materials. The Brunauer-Emmett-Teller (BET) surface area was calculated to be 9.197 and 25.998  $m^2 g^{-1}$  for Alg/PVA NFs 2:8 and Alg/PVA/Z NFs 2:8:2.5, respectively. Zeolites porous structure increased specific surface area of the nanofibers and provided more active sites to capture  $CO_2$  molecules. Consequently, at a relatively similar basis weight, Alg/PVA/Z NFs showed over than three times bigger adsorption capacity compared to Alg/PVA NFs.

### Interaction between Alginate-Based Nanofibers and Carbon Dioxide

Alginate binds  $CO_2$  through the carboxyl and hydroxyl groups within the chains [24]. Besides,  $CO_2$  also can interact with the carbonyl group of PVA. The electron pair of the polymers carbonyl oxygen interacts with the carbon atom of carbon dioxide, in which the carbon atom of  $CO_2$  molecules acts as an electron acceptor and lone pair electron of polymer carbonyl oxygen acts as an electron donor species [44]. FTIR spectra (Fig. 12) showed that after  $CO_2$  adsorption, the carbonyl ( $1095\text{ cm}^{-1}$ ) and symmetric carboxyl ( $1427\text{ cm}^{-1}$ ) peaks of Alg/PVA NFs disappeared, also asymmetric  $-COO-$  and  $-OH$  stretching vibration shifted to higher wavenumber. The few changed peaks in FTIR spectra showed that Alg/PVA NFs binds  $CO_2$  *via* hydrogen bond and Lewis acid-base interaction. There were two suggested configurations of Lewis acid-base interaction between polymers carbonyl groups and  $CO_2$ : T-shaped geometry and bent T-shaped configuration [44].

Zeolites attract strongly to the gases with high quadrupole moment such as carbon dioxide *via* electric field produced by the cation of the zeolites. Interaction between zeolites framework structure and  $CO_2$  molecules involved relatively weak intermolecular forces, namely Van der Waal's forces and electrostatic interaction [27,40,45].

### Adsorption Isotherm Studies

The adsorption behaviors of alginate-based nanofibers were analyzed using Langmuir, Freundlich,

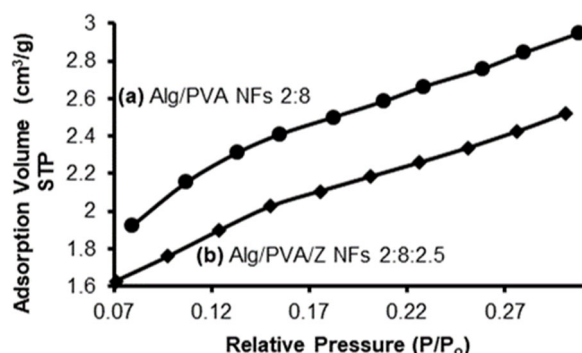


Fig 12.  $N_2$  adsorption/desorption isotherm for  $CO_2$  onto Alg/PVA NFs 2:8 (a) and Alg/PVA/Z NFs 2:8:2.5 (b)

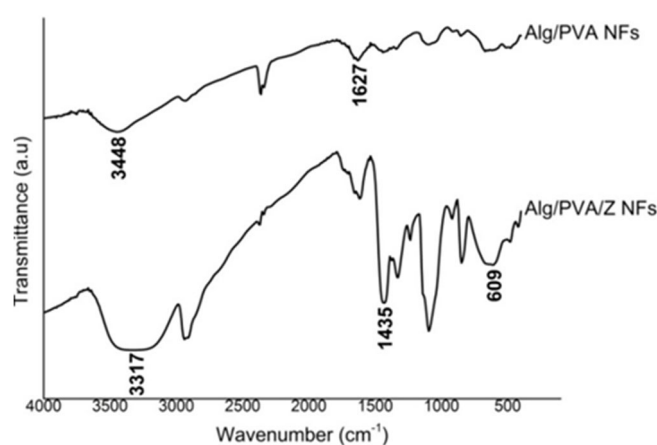


Fig 13. FTIR spectra of Alg/PVA NFs 2:8 and Alg/PVA/Z NFs 2:8:2.5 after  $CO_2$  adsorption

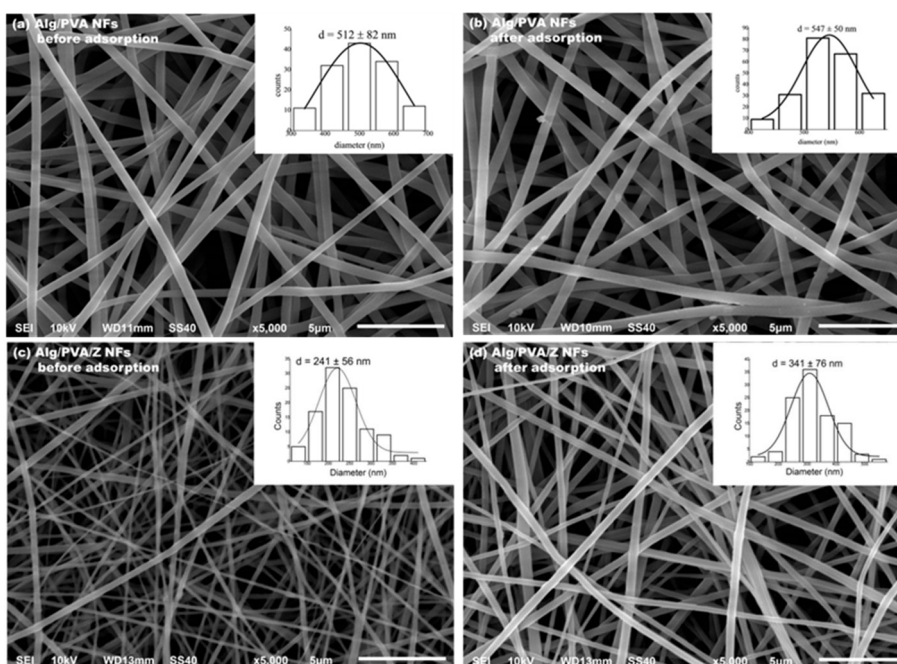
Temkin, Dubinin-Radushkevich (DR), and Elovich isotherm models [46]. See Table S2 for the detailed equations and curve plots.

Table 1 shows the result parameters and correlation coefficients ( $R^2$ ) of each isotherm mode, a measure of goodness-of-fit, representing good linearity for a certain model relative to the other models. Plot  $C_e$  versus  $C_e/q_e$  of Alg/PVA NFs 2:8 gives the highest  $R^2$  value (0.9999), revealing that Alg/PVA NFs 2:8 were fit the Langmuir isotherm model. Langmuir Isotherm is primarily designed to describe gas-solid phase adsorption. This isotherm was based on the assumption that  $CO_2$  adsorption occurred on the homogeneous surface of Alg/PVA NFs 2:8 by monolayer sorption [46].

On the other hands, carbon dioxide adsorption onto Alg/PVA/Z NFs 2:8:2.5 showed good fitness of Dubinin-Radushkevich (DR) isotherm model as the plot of  $\epsilon^2$  versus  $\ln q_e$  gives correlation efficient value close to

**Table 1.** Isotherm parameters for adsorption of CO<sub>2</sub> onto alginate-based nanofibers

Models	Parameters	Alg/PVA NFs	Alg/PVA/Z NFs
Langmuir	$K_L$ , mmol <sup>-1</sup>	-447.2222	1.3239
	$q_m$ , mmol g <sup>-1</sup>	2.484	12.6103
	$R^2$	0.9999	0.5923
Freundlich	$K_F$ , mmol g <sup>-1</sup> mmol <sup>-1/n</sup>	1.3971	4.0435
	$n$	-12.7551	1.3770
	$R^2$	0.8641	0.9065
DR	$K_{DR}$ , mol <sup>2</sup> kJ <sup>-2</sup>	$-2 \times 10^{-9}$	$5 \times 10^{-8}$
	$q_s$ , mmol g <sup>-1</sup>	2.3936	7.2355
	$R^2$	0.904	0.9168
Temkin	$K_T$ , mmol <sup>-1</sup>	0.9998	1.0071
	$b_T$	$-1.1031 \times 10^4$	$9.5449 \times 10^2$
	$R^2$	0.8527	0.8965
Elovich	$K_E$	3.4060	-1.6955
	$q_m$ , mmol g <sup>-1</sup>	-0.2414	14.8148
	$R^2$	0.8725	0.2647

**Fig 14.** Morphological changes of Alg/PVA NFs 1:9 (a, b) and Alg/PVA/Z NFs 2:8:1.5 (c, d) before and after the adsorption process; insets show diameter of each nanofibers

unity. DR isotherm model is an empirical adsorption model that is generally applied to express adsorption mechanism with Gaussian energy distribution onto heterogeneous surfaces. The model was a semiempirical equation in which CO<sub>2</sub> adsorption follows a pore-filling mechanism through multilayer character involving Van

der Waal's forces of CO<sub>2</sub> gases on microporous zeolites inside Alg/PVA/Z NFs 2:8:2.5 [46].

### Reusability of Alginate-Based Nanofibers

To understand the spontaneity of the adsorption process, the Gibbs free energy was calculated using the

following Eq. (1).

$$\Delta G^\circ = -RT \ln K_L \quad (1)$$

where  $\Delta G^\circ$  is Gibbs free energy ( $\text{kJ mol}^{-1}$ ),  $R$  is gas constant ( $8.314 \text{ J mol}^{-1} \text{ K}^{-1}$ ),  $T$  is the temperature (K), and  $K_L$  is Langmuir equilibrium constant. The result showed that the  $\Delta G^\circ$  values of Alg/PVA NFs 2:8 were  $1.108 \text{ kJ mol}^{-1}$ , obtained below  $20 \text{ kJ mol}^{-1}$ . These findings suggest that the  $\text{CO}_2$  adsorption was followed by the physisorption mechanism [40].

Energy adsorption of Alg/PVA/Z NFs 2:8:2.5 could be calculated by the following equation:

$$E = \frac{1}{\sqrt{2K_{DR}}} \quad (2)$$

where  $E$  is energy adsorption ( $\text{kJ mol}^{-1}$ ), and  $K_{DR}$  is Dubinin-Radushkevich equilibrium constant ( $\text{mol}^2 \text{ kJ}^{-2}$ ). The value of  $E$  for Alg/PVA/Z NFs 2:8:2.5 were lower than  $8 \text{ kJ mol}^{-1}$  ( $E = 3.162 \text{ kJ mol}^{-1}$ ). The calculated  $E$  represented the physical nature of the sorption [47]. Fig. 13 showed SEM images of alginate-based nanofibers and  $\text{CO}_2$  adsorbed alginate-based nanofibers. All images displayed relatively unchanging surface morphology as well as diameter of the nanofibers (see the inset of Fig. 13).

## ■ CONCLUSION

Alginate is not able to electrospun from aqueous solutions because it possesses a polyelectrolyte characteristic. However, incorporating copolymer poly (vinyl alcohol) (PVA) 10% (w/w) into alginate solution (2% w/w) weakens the repulsive forces among polyanionic alginate chains, thus enabling alginate nanofibers formation. Alg/PVA NFs with uniform, continuous, smooth-surfaced nanofibers were obtained from Alg:PVA solution volume ratio 2:8 with average diameter of  $202 \pm 43 \text{ nm}$  and specific surface area of  $9.197 \text{ m}^2 \text{ g}^{-1}$ . The Alg/PVA NFs for  $\text{CO}_2$  capture was evaluated using a gas trapping system. The maximum adsorption capacity was  $3.286 \text{ mmol g}^{-1}$ , conducted within optimum conditions at flow rate and contact time about  $20 \text{ mL min}^{-1}$  and 20 min, respectively. To improve the properties and performances of alginate nanofibers, zeolite particles were impregnated into polymers solution. Impregnated zeolites altered nanofibers surface morphologies from smooth to rough fiber with an average

diameter of  $250 \pm 60 \text{ nm}$  and enhanced specific surface area to  $25.998 \text{ m}^2 \text{ g}^{-1}$ . The optimum  $\text{CO}_2$  adsorption capacity of Alg/PVA/Z NFs was  $10.710 \text{ mmol g}^{-1}$ . The adsorption behavior of resulting nanofibers was studied using five different isotherm models. Alg/PVA NFs showed the best linearity with Langmuir isotherm model with  $R^2$  0.9999, and Alg/PVA/Z NFs was fit with in Dubinin-Radushkevich (DR) isotherm model. SEM images of nanofibers before and after the adsorption process displayed unchanging surface morphologies as well as the diameter of the nanofibers. The result of this study suggested that Alg/PVA NFs and Alg/PVA/Z NFs are promising candidates for  $\text{CO}_2$  capture with high adsorption capacity that can be fabricated from eco-friendly and low-cost raw materials.

## ■ ACKNOWLEDGMENTS

The research was supported by the Ministry of Research, Technology and Higher Education of Indonesia under PUPT Project Grand No. 745/UN1-P/LT/DIT-LIT/2016.

## ■ REFERENCES

- [1] NOAA/ESRL, 2022, National Oceanic & Atmospheric Administration (NOAA)/Earth System Research Laboratory (ESRL) - Trends in Atmospheric Carbon Dioxide, <https://gml.noaa.gov/ccgg/trends/global.html>, accessed on March 22, 2022.
- [2] Hussin, F., and Aroua, M.K., 2020, Recent trends in the development of adsorption technologies for carbon dioxide capture: A brief literature and patent reviews (2014–2018), *J. Cleaner Prod.*, 253, 119707.
- [3] Xue, J., Wu, T., Dai, Y., and Xia, Y., 2019, Electrospinning and electrospun nanofibers: Methods, materials, and applications, *Chem. Rev.*, 119 (8), 5298–5415.
- [4] Marin, L., Dragoi, B., Olaru, N., Perju, E., Coroaba, A., Doroftei, F., Scavia, G., Destri, S., Zappia, S., and Porzio, W., 2019, Nanoporous furfuryl-imine-chitosan fibers as a new pathway towards eco-materials for  $\text{CO}_2$  adsorption, *Eur. Polym. J.*, 120, 109214.

- [5] Jiamjirangkul, P., Inprasit, T., Intasanta, V., and Pagon, A., 2020, Metal organic framework-integrated chitosan/poly(vinyl alcohol) (PVA) nanofibrous membrane hybrids from green process for selective CO<sub>2</sub> capture and filtration, *Chem. Eng. Sci.*, 221, 115650.
- [6] Lin, Y.F., Ye, Q., Hsu, S.H., and Chung, T.W., 2016, Reusable fluorocarbon-modified electrospun PDMS/PVDF nanofibrous membranes with excellent CO<sub>2</sub> absorption performance, *Chem. Eng. J.*, 284, 888–895.
- [7] Zainab, G., Iqbal, N., Babar, A.A., Huang, C., Wang, X., Yu, J., and Ding, B., 2017, Free-standing, spider-web-like polyamide/carbon nanotube composite nanofibrous membrane impregnated with polyethyleneimine for CO<sub>2</sub> capture, *Compos. Commun.*, 6, 41–47.
- [8] Olivieri, L., Roso, M., De Angelis, M.G., and Lorenzetti, A., 2018, Evaluation of electrospun nanofibrous mats as materials for CO<sub>2</sub> capture: a feasibility study on functionalized poly(acrylonitrile) (PAN), *J. Membr. Sci.*, 546, 128–138.
- [9] Zainab, G., Babar, A.A., Iqbal, N., Wang, X., Yu, J., and Ding, B., 2018, Amine-impregnated porous nanofiber membranes for CO<sub>2</sub> capture, *Compos. Commun.*, 10, 45–51.
- [10] Hong, S.M., Kim, S.H., Jeong, B.G., Jo, S.M., and Lee, K.B., 2014, Development of porous carbon nanofibers from electrospun polyvinylidene fluoride for CO<sub>2</sub> capture, *RSC Adv.*, 4 (103), 58956–58963.
- [11] Nan, D., Liu, J., and Ma, W., 2015, Electrospun phenolic resin-based carbon ultrafine fibers with abundant ultra-small micropores for CO<sub>2</sub> adsorption, *Chem. Eng. J.*, 276, 44–50.
- [12] Heo, Y.J., Zhang, Y., Rhee, K.Y., and Park, S.J., 2019, Synthesis of PAN/PVDF nanofiber composites-based carbon adsorbents for CO<sub>2</sub> capture, *Composites, Part B*, 156, 95–99.
- [13] Chiang, Y.C., Wu, C.Y., Chen, Y.J., 2020, Effects of activation on the properties of electrospun carbon nanofibers and their adsorption performance for carbon dioxide, *Sep. Purif. Technol.*, 233, 116040.
- [14] Zainab, G., Babar, A.A., Ali, N., Aboalhassan, A.A., Wang, X., Yu, J., and Ding, B., 2020, Electrospun carbon nanofibers with multi-aperture/opening porous hierarchical structure for efficient CO<sub>2</sub> adsorption, *J. Colloid Interface Sci.*, 561, 659–667.
- [15] Zhang, Y., Zhang, Y., Wang, X., Yu, J., and Ding, B., 2018, Ultrahigh metal-organic framework loading and flexible nanofibrous membranes for efficient CO<sub>2</sub> capture with long-term, ultrastable recyclability, *ACS Appl. Mater. Interfaces*, 10 (40), 34802–34810.
- [16] Choi, C., Kadam, R.L., Gaikwad, S., Hwang, K.S., and Han, S., 2020, Metal organic frameworks immobilized polyacrylonitrile fiber mats with polyethyleneimine impregnation for CO<sub>2</sub> capture, *Microporous Mesoporous Mater.*, 296, 110006.
- [17] Zhang, Y., Guan, J., Wang, X., Yu, J., and Ding, B., 2017, Balsam-pear-skin-like porous polyacrylonitrile nanofibrous membranes grafted with polyethyleneimine for postcombustion CO<sub>2</sub> capture, *ACS Appl. Mater. Interfaces*, 9 (46), 41087–41098.
- [18] Abbasi, A., Nasef, M.M., Kheawhom, S., Faridi-Majidi, R., Takeshi, M., Abouzari-Lotf, E., and Choong, T., 2019, Amine functionalized radiation induced grafted polyolefin nanofibers for CO<sub>2</sub> adsorption, *Radiat. Phys. Chem.*, 156, 58–66.
- [19] Iqbal, N., Wang, X., Babar, A.A., Yu, J., and Ding, B., 2016, Highly flexible NiCo<sub>2</sub>O<sub>4</sub>/CNTs doped carbon nanofibers for CO<sub>2</sub> adsorption and supercapacitor electrodes, *J. Colloid Interface Sci.*, 476, 87–93.
- [20] Ali, N., Babar, A.A., Zhang, Y., Iqbal, N., Wang, X., Yu, J., and Ding, B., 2020, Porous, flexible, and core-shell structured carbon nanofibers hybridized by tin oxide nanoparticles for efficient carbon dioxide capture, *J. Colloid Interface Sci.*, 560, 379–387.
- [21] Jain, R., Shetty, S., and Yadav, K.S., 2020, Unfolding the electrospinning potential of biopolymers for preparation of nanofibers, *J. Drug Delivery Sci. Technol.*, 57, 101604.
- [22] FAO, 2018, *The Global Status of Seaweed Production, Trade and Utilization*, Globefish

- Research Programme, Volume 124, Food Agriculture Organization, Rome.
- [23] Anonymous, 2019, *Peraturan Presiden Republik Indonesia No. 3 Tahun 2019 tentang Peta Panduan (Road map) Pengembangan Industri Rumput Laut Nasional Tahun 2018-2021*, Ministry of State Secretariat of the Republic of Indonesia, Jakarta.
- [24] Zhu, Y., Wang, Z., Zhang, C., Wang, J., and Wang, S., 2013, A novel membrane prepared from sodium alginate cross-linked with sodium tartrate for CO<sub>2</sub> capture, *Chin. J. Chem. Eng.*, 21 (10), 1098–1105.
- [25] Rošić, R., Pelipenko, J., Kocbek, P., Baumgartner, S., Bešter-Rogač, M., and Kristl, J., 2012, The role of rheology of polymer solutions in predicting nanofiber formation by electrospinning, *Eur. Polym. J.*, 48 (8), 1374–1384.
- [26] Mirtič, J., Balažić, H., Zupančič, Š., and Kristl, J., 2019, Effect of solution composition variables on electrospun alginate nanofibers: Response surface analysis, *Polymers*, 11, 692.
- [27] Abd, A.A., Naji, S.Z., Hashim, A.S., and Othman, M.R., 2020, Carbon dioxide removal through physical adsorption using carbonaceous and non-carbonaceous adsorbents: A review, *J. Environ. Chem. Eng.*, 8 (5), 104142.
- [28] Kim, H.G., and Kim, J.H., 2011, Preparation and properties of antibacterial poly(vinyl alcohol) nanofibers by nanoparticles, *Fibers Polym.*, 12 (5), 602.
- [29] Nawawi, M.S., Ahmad, M.R., Affandi, N.D.N., Sekak, K.A., and Ahmad, W.Y.W., 2013, Effect of zeolite presence and voltage variance on the fiber diameter of microporous PVA/zeolite nanofibrous membrane, *2013 IEEE Business Engineering and Industrial Applications Colloquium (BEIAC 2013)*, Institute of Electrical and Electronics Engineers (IEEE) Langkawi, Malaysia, 344–348.
- [30] Kang, D.H., and Kang, H.W., 2016, Surface energy characteristics of zeolite embedded PVDF nanofiber films with electrospinning process, *Appl. Surf. Sci.*, 387, 82–88.
- [31] Anis, S.F., and Hashaikeh, R., 2016, Electrospun zeolite-Y fibers: Fabrication and morphology analysis, *Microporous Mesoporous Mater.*, 233, 78–86.
- [32] Anis, S.F., Khalil, A., Saepurahman, Singaravel, G., and Hashaikeh, R., 2016, A review on the fabrication of zeolite and mesoporous inorganic nanofibers formation for catalytic applications, *Microporous Mesoporous Mater.*, 236, 176–192.
- [33] Bahi, A., Shao, J., Mohseni, M., and Ko, F.K., 2017, Membranes based on electrospun lignin-zeolite composite nanofibers, *Sep. Purif. Technol.*, 187, 207–213
- [34] Habiba, U., Afifi, A.M., Salleh, A., and Ang, B.C., 2017, Chitosan/(polyvinyl alcohol)/zeolite electrospun composite nanofibrous membrane for adsorption of Cr<sup>6+</sup>, Fe<sup>3+</sup> and Ni<sup>2+</sup>, *J. Hazard. Mater.*, 322, 182–194.
- [35] Ji, S.H., Cho, J.H., Jeong, Y.H., Yun, J.D., and Yun, J.S., 2017, The synthesis of flexible zeolite nanofibers by a polymer surface thermal etching process, *Appl. Surf. Sci.*, 416, 178–182.
- [36] Ojstršek, A., Fakin, D., Hribernik, S., Fakin, T., Bračić, M., and Kurečić, M., 2020, Electrospun nanofibrous composites from cellulose acetate/ultra-high silica zeolites and their potential for VOC adsorption from air, *Carbohydr. Polym.*, 236, 116071.
- [37] Islam, M.S., and Karim, M.R., 2010, Fabrication and characterization of poly(vinyl alcohol)/alginate blend nanofibers by electrospinning method, *Colloids Surf., A*, 366 (1-3), 135–140.
- [38] Shalumon, K.T., Anulekha, K.H., Nair, S.V., Nair, S.V., Chennazhi, K.P., and Jayakumar, R., 2011, Sodium alginate/poly(vinyl alcohol)/nano ZnO composite nanofibers for antibacterial wound dressings, *Int. J. Biol. Macromol.*, 49 (3), 247–254.
- [39] Mozgawa, W., Król, M., and Barczyk, K., 2011, FT-IR studies of zeolites from different structural groups, *Chemik*, 65 (7), 671–674.
- [40] Pham, T.H., Lee, B.K., Kim, J., and Lee, C.H., 2016, Enhancement of CO<sub>2</sub> capture by using synthesized nano-zeolite, *J. Taiwan Inst. Chem. Eng.*, 64, 220–226.

- [41] Pelipenko, J., Kocbek, P., and Kristl, J., 2015, Critical attributes of nanofibers: Preparation, drug loading, and tissue regeneration, *Int. J. Pharm.*, 484 (1-2), 57–74.
- [42] Balgis, R., Kartikowati, C.W., Ogi, T., Gradon, L., Bao, L., Seki, K., and Okuyama, K., 2015, Synthesis and evaluation of straight and bead-free nanofibers for improved aerosol filtration, *Chem. Eng. Sci.*, 137, 947–954.
- [43] Matulevicius, J., Kliucininkas, L., Martuzevicius, D., Krugly, E., Tichonovas, M., and Baltrusaitis, J., 2014, Design and characterization of electrospun polyamide nanofiber media for air filtration applications, *J. Nanomater.*, 2014, 859656.
- [44] Kazarian, S.G., Vincent, M.F., Bright, F.V., Liotta, C.L., and Eckert, C.A., 1996, Specific intermolecular interaction of carbon dioxide with polymers, *J. Am. Chem. Soc.*, 118 (7), 1729–1736.
- [45] Zhao, L., Chen, Y., Wang, B., Sun, C., Chakraborty, S., Ramasubramanian, Dutta, P.K., and Ho, W.S.W., 2016, Multilayer polymer/zeolite Y composite membrane structure for CO<sub>2</sub> capture from flue gas, *J. Membr. Sci.*, 498, 1–13.
- [46] Ayawei, N., Ebelegi, A.N., and Wankasi, D., 2017, Modelling and interpretation of adsorption isotherms, *J. Chem.*, 2017, 3039817.
- [47] Raganati, F., Alfe, M., Gargiulo, V., Chirone, R., and Ammendola, P., 2018, Isotherms and thermodynamics of CO<sub>2</sub> adsorption on a novel carbon-magnetite composite sorbent, *Chem. Eng. Res. Des.*, 134, 540–552.